

Parton distributions in the valon modelRudolph C. Hwa¹ and C. B. Yang^{1,2}¹*Institute of Theoretical Science and Department of Physics, University of Oregon, Eugene, Oregon 97403-5203*²*Institute of Particle Physics, Hua-Zhong Normal University, Wuhan 430079, People's Republic of China*

(Received 18 February 2002; published 27 August 2002)

The parton distribution functions determined by CTEQ at low Q^2 are used as inputs to test the validity of the valon model. The valon distributions in a nucleon are first found to be nearly Q independent. The parton distributions in a valon are shown to be consistent with being universal, independent of the valon type. The momentum fractions of the partons in the valon add up separately to one. These properties affirm the validity of the valon model. The various distributions are parametrized for convenient application of the model.

DOI: 10.1103/PhysRevC.66.025204

PACS number(s): 12.39.Ki, 13.85.Ni, 24.85.+p

I. INTRODUCTION

The parton distributions in proton have been studied extensively in recent years over wide ranges of Q^2 and x [1–3]. For example, in the CTEQ global analysis framework [1], the distribution functions have been determined by fitting some 1300 data points obtained for various reactions in 16 experiments; over 30 parameters are used in the input parton distribution functions (PDFs) in the next-to-leading-order calculations in perturbative QCD [4]. The results on the PDFs at various Q^2 are presented in the form of graphs available on the web [5]. The distribution functions are accurately calculated numerically, but they are inconvenient to describe analytically. The purpose of this paper is twofold. One is to provide a simple parametrization of the parton distribution functions, which is accurate to within 5% for $1 < Q^2 < 100$ (GeV/c)² and $10^{-2} < x < 1$. The other is to provide firm evidence for the validity of a model that can be very useful in the study of soft processes in hadronic and nuclear collisions.

The model under discussion is the valon model [6,7]. Valons play a role in scattering problems as the constituent quarks do in bound-state problems. In the model it is assumed that the valons stand at a level in between hadrons and partons and that the structure of a hadron in terms of the valons is independent of Q^2 . That is, the property that a nucleon has three valons that carry all the momentum of the nucleon does not change with Q^2 . Each valon may be viewed as a parton cluster associated with one and only one valence quark, so the flavor quantum numbers of a valon are those of a valence quark. The Q^2 evolution of the parton distributions in a nucleon is effected through the evolution of the valon structure, as the higher resolution of a probe reveals the parton content of the valons.

When the valon model was first proposed, the deep inelastic scattering data was not precise enough either to rule out the model or to determine accurately the parameters in the model. One may regard the situation then as one in which the model satisfies the sufficiency condition for an approximate description of the nucleon structure, but not necessary. Now, the experimental data have vastly improved and the PDFs have been so precisely determined that the validity of the valon model can be put to a stringent test. That is what we intend to do in this paper. Although no model is ever neces-

sary in the mathematical sense, we shall show that the concept of valons as constituents of the nucleon is eminently acceptable by virtue of the Q^2 independence of the valon distribution functions, the universality of the parton distributions in valons, and the momentum sum rule of the partons in a valon being satisfied.

In terms of the parametrization in the valon model the parton distributions are much simpler to describe, and therefore more convenient to transport to different problems. Our focus will be on soft processes at low Q^2 , for which perturbative QCD is inapplicable. The valon picture then provides a systematic way of organizing various contributions to inclusive processes. For example, the quark-antiquark joint distribution functions can be unambiguously calculated in the valon model. Such distribution functions are needed for the determination of the pion inclusive cross section in the framework of the recombination model [8].

In a broader perspective of the hadron structure problem, let us comment on where the valon model fits in the general picture. There are two commonly accepted views of the hadron structure. One is the static problem of the hadrons in terms of the constituent quarks (CQs). In that picture the wave functions of the CQs are determined; they describe the various bound states of the confining potential. The other is the deep inelastic scattering problem in which the hadron (mainly proton) is probed in high- Q^2 processes and the various PDFs are determined. The two pictures are complementary, but neither gives any hint of the other. The CQs give no insight into the role of the gluons, and the PDFs give no clue that a proton is made of three CQs. It is in the valon model that the two pictures are unified. Moreover, the two pictures have such restricted domains of applicability that they provide very little insight on the dominant features of multiparticle production in hadronic collisions. The inclusive cross sections of produced hadrons are sensitively dependent on the hadron structure, since it is known that $xd\sigma/dx$ at low p_T for pions, say, produced in the proton fragmentation region is very different from that in the pion fragmentation region. The two aforementioned pictures of the hadron structure offer no clear explanation why this is so. The valon model makes possible the calculation of the inclusive distributions [9,10]. Indeed, the determination of the nondiffractive inclusive cross sections is an essential sequel to the present paper, because it exhibits the predictive power of the valon model.

In this paper we prepare the ground for that application [10] by unifying the CQ picture with the PDFs of the hadrons and by determining some essential parameters in the valon model.

Since the CQ model and the PDFs describe widely different kinematic regions, we can unify them only in the domain where we can find some degree of overlap. For that reason we limit ourselves to the region $1 < Q^2 < 100$ (GeV/c)². We do not go lower in Q^2 , since the lowest PDFs given by CTEQ4LQ is $Q^2 = 1$ (GeV/c)² [5]. Without going too high in Q^2 that is the proper domain of perturbative QCD, we also refrain from going too low in x . Our choice of limiting ourselves to $x > 0.01$ relieves us from putting heavy burden on the accuracy of the CTEQ4LQ input at smaller x and low Q^2 . The kinematic range for the determination of our valon-model parameters is totally adequate for the type of applications we envisage for the model. In addition to applying the model to hadronic collisions [10], we have already considered the application to proton-nucleus collisions [11], but without the benefit of the parameters determined in this paper, we used only the old parameters based on outdated experiments. Nevertheless, in the framework of the valon model we have been able to determine the nature of momentum degradation of produced nucleons as a function of the target nuclear size. That is an important first step towards understanding baryon stopping in heavy-ion collisions. The parameters to be determined in this paper are needed to improve the numerical details of the momentum degradation problem in proton-nucleus collisions, but not the general features and qualitative properties of the problem.

II. THE VALON MODEL

In the valon model we assume that a proton consists of three valons (UUD) that separately contain the three valence quarks (uud). Let the exclusive valon distribution function be

$$G_{UUD}(y_1, y_2, y_3) = g(y_1 y_2)^\alpha y_3^\beta \delta(y_1 + y_2 + y_3 - 1), \quad (1)$$

where y_i are the momentum fractions of the U valons ($i = 1, 2$) and D valon ($i = 3$). The variable y will never refer to rapidity in this paper. The normalization factor g is determined by the requirement that the probability for the proton to consist three and only three valons is 1, i.e.,

$$\int_0^1 dy_1 \int_0^{1-y_1} dy_2 \int_0^{1-y_1-y_2} dy_3 G_{UUD}(y_1, y_2, y_3) = 1. \quad (2)$$

Note that the valon distribution function is not defined in the invariant phase space. From Eq. (2) we have

$$g = [B(\alpha + 1, \beta + 1) B(\alpha + 1, \alpha + \beta + 2)]^{-1}, \quad (3)$$

where $B(m, n)$ is the beta function. The single-valon distributions are

$$\begin{aligned} G_U(y) &= \int_0^{1-y} dy_2 \int_0^{1-y-y_2} dy_3 G_{UUD}(y, y_2, y_3) \\ &= g B(\alpha + 1, \beta + 1) y^\alpha (1-y)^{\alpha + \beta + 1}, \end{aligned} \quad (4)$$

$$\begin{aligned} G_D(y) &= \int_0^{1-y} dy_1 \int_0^{1-y-y_1} dy_2 G_{UUD}(y_1, y_2, y) \\ &= g B(\alpha + 1, \alpha + 1) y^\beta (1-y)^{2\alpha + 1}. \end{aligned} \quad (5)$$

An essential property of the valon model is that the structure of the proton in terms of the valons is independent of the probe. It means that when probed at high Q^2 , whatever the experiment may be, the parton distributions in a proton can be expressed as a convolution of the valon distribution and the parton distribution in a valon, i.e.,

$$\begin{aligned} x u(x, Q^2) &= \int_x^1 dy [2G_U(y)K(x/y, Q^2) \\ &\quad + G_D(y)L_u(x/y, Q^2)], \end{aligned} \quad (6)$$

$$\begin{aligned} x d(x, Q^2) &= \int_x^1 dy [G_D(y)K(x/y, Q^2) \\ &\quad + 2G_U(y)L_u(x/y, Q^2)], \end{aligned} \quad (7)$$

where $u(x, Q^2)$ and $d(x, Q^2)$ are the u and d quark distributions, respectively, and x the momentum fraction of the quark. We emphasize that on the right-hand side (RHS) of the above equations the Q^2 dependences appear only in parton distributions in the valons, $K(z, Q^2)$ and $L_u(z, Q^2)$, but not in the valon distributions $G_U(y)$ and $G_D(y)$. We regard this as the defining property of the valon model. In that sense the model is analogous to the one in which a deuteron is treated as a bound state of two nucleons; in that treatment a high- Q^2 probe resolves the structure of one or the other nucleon without affecting the nucleon wave function of the deuteron.

There are two types of parton distributions in the valons, which appear in Eqs. (6) and (7). $K(z, Q^2)$ refers to the favored partons, i.e., u in U and d in D , whereas $L_u(z, Q^2)$ refers to the unfavored partons, i.e., u in D and d in U . The distribution $K(z, Q^2)$ can be further divided into two types,

$$K(z, Q^2) = K_{NS}(z, Q^2) + L_f(z, Q^2), \quad (8)$$

where the first term on the RHS is the valence quark distribution (hence, nonsinglet), while the second is the sea quark distribution for the same flavor type. Since the sea quarks should respect charge conjugation invariance, the u and \bar{u} in the sea (and similarly d and \bar{d}) have the same distributions, i.e.,

$$\begin{aligned} x \bar{u}(x, Q^2) &= \int_x^1 dy [2G_U(y)L_f(x/y, Q^2) \\ &\quad + G_D(y)L_u(x/y, Q^2)], \end{aligned} \quad (9)$$

$$x \bar{d}(x, Q^2) = \int_x^1 dy [G_D(y) L_f(x/y, Q^2) + 2G_U(y) L_u(x/y, Q^2)]. \quad (10)$$

The valence quark distributions are then

$$x u_v(x, Q^2) = \int_x^1 dy 2G_U(y) K_{NS}(x/y, Q^2), \quad (11)$$

$$x d_v(x, Q^2) = \int_x^1 dy G_D(y) K_{NS}(x/y, Q^2). \quad (12)$$

In earlier treatments [6–11] L_f and L_u have been regarded as identical due to the assumption of the symmetric sea. Indeed, putting $L_f = L_u$ in Eqs. (9) and (10) results in $\bar{u}(x, Q^2) = \bar{d}(x, Q^2)$, which is a necessary consequence of the sea quarks satisfying SU(2) symmetry. However, there is experimental evidence [12] that Gottfried integral $\int (F_2^p - F_2^n) dx/x$ is less than 1/3, which is the value expected in the simple quark model. Thus we should allow L_f to be different from L_u . Indeed, in the valon model we may expect that in a U valon the necessary presence of a u valence quark would, on the grounds of Fermi statistics, make a gluon have more difficulty converting virtually into a $u\bar{u}$ pair than into a $d\bar{d}$ pair. Hence, L_f should be suppressed relative to L_u . Since there are two U and one D in a proton, we should expect the overall \bar{u} to be less than \bar{d} . The data do indicate $\bar{u} < \bar{d}$ after integration over x [12]. We thus see that the breaking of SU(2) in the sea is related to Pauli blocking in the valons.

III. THE VALON DISTRIBUTIONS

The valence quark distributions, u_v and d_v , are given by CTEQ4LQ [5]. From Eqs. (11) and (12) we see that they are directly related to the valon distributions $G_U(y)$ and $G_D(y)$ by convolutions with the common factor K_{NS} . It is therefore possible to isolate the valon distributions by deconvolution using the moments. Let us define

$$\tilde{G}_{U,D}(n) = \int_0^1 dy y^{n-1} G_{U,D}(y), \quad (13)$$

$$\tilde{K}_{NS}(n, Q^2) = \int_0^1 dz z^{n-2} K_{NS}(z, Q^2), \quad (14)$$

$$\tilde{u}_v(n, Q^2) = \int_0^1 dx x^{n-1} u_v(x, Q^2), \quad (15)$$

and similarly for \tilde{d}_v in terms of d_v . Then by the convolution theorem we have from Eqs. (11) and (12),

$$\tilde{u}_v(n, Q^2) = 2\tilde{G}_U(n) \tilde{K}_{NS}(n, Q^2), \quad (16)$$

$$\tilde{d}_v(n, Q^2) = \tilde{G}_D(n) \tilde{K}_{NS}(n, Q^2). \quad (17)$$

It thus follows that

$$\frac{\tilde{G}_U(n)}{\tilde{G}_D(n)} = \frac{\tilde{u}_v(n, Q^2)}{2\tilde{d}_v(n, Q^2)}. \quad (18)$$

If the valon model is valid, then the LHS is Q^2 independent, a property that we can check directly by examining the Q^2 dependence of the RHS. Since $u_v(x, Q^2)$ and $d_v(x, Q^2)$ can separately be determined from Ref. [5], we only have to take their moments and calculate their ratio.

To do the above analysis, we have to set the range of Q^2 to be examined, since the valon model is not expected to be accurate for all Q^2 . As we have discussed near the end of Sec. I, the valon model has been applied to soft production problems because they involve nonperturbative processes. For hard processes at very high $Q^2 [Q^2 > 100 (\text{GeV}/c)^2]$, perturbative QCD is very successful and there is no need to introduce any inaccuracy through the use of a model. We shall therefore limit ourselves to the range $1 < Q^2 < 100 (\text{GeV}/c)^2$. This is actually a very wide range for hadronic processes that can involve the production of soft particles and semihard minijets.

For the range of Q^2 chosen we must use low- Q^2 parametrization of the PDFs. CTEQ4LQ [5] gives the graphs of u , d , s , \bar{u} , \bar{d} , and g distributions at any Q evolved from the starting scale at $Q_0^2 = 0.49 (\text{GeV}/c)^2$. Since u_v and d_v distributions are not included in the list of PDFs posted, we have to calculate

$$u_v(x, Q^2) = u(x, Q^2) - \bar{u}(x, Q^2), \quad (19)$$

$$d_v(x, Q^2) = d(x, Q^2) - \bar{d}(x, Q^2), \quad (20)$$

from the q and \bar{q} graphs for the RHS available from the web. We extract the numerical values at up to 60 points of x values per PDF for three values of Q : 1, 3, and 10 GeV/ c . From the values of u_v and d_v thus determined, we then compute the moments in accordance to Eq. (15) for $n = 2, \dots, 9$. Denoting the RHS of Eq. (18) by $r(n, Q)$ we then calculate the ratio of ratios

$$R(n, Q) = r(n, Q) / r(n, Q = 1) \quad (21)$$

relative to $Q = 1$ GeV/ c . Figure 1 shows how $R(n, Q)$ depends on n for $Q = 3$ and 10 GeV/ c . It is evident that the dependence is very mild, the maximum deviation from 1 being around 7% at $n = 9$ and $Q = 10$ GeV/ c . We regard this approximate constancy of $R(n, Q)$, while Q is increased by an order of magnitude, as the first step towards a confirmation of the validity of the valon model. That is, the insensitivity of $R(n, Q)$ to Q variation supports our assumption that $\tilde{G}_U(n) / \tilde{G}_D(n)$ is Q independent to a degree sufficient for the application of the valon model.

The n dependence of $r(n, Q) = \tilde{u}_v(n, Q) / 2\tilde{d}_v(n, Q)$, as determined from the CTEQ4LQ data, can now be used to fix the parameters α and β in the valon distributions. From Eqs. (4), (5), and (13), we have

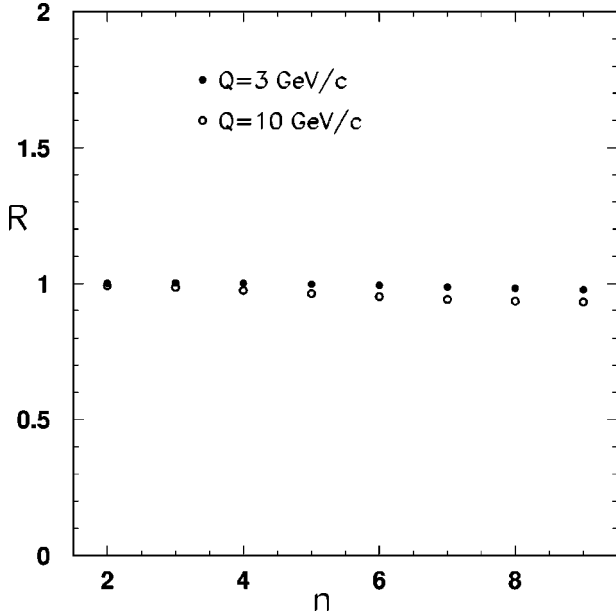


FIG. 1. The ratio of ratios defined in Eq. (21).

$$\tilde{G}_U(n) = B(\alpha+n, \alpha+\beta+2)/B(\alpha+1, \alpha+\beta+2), \quad (22)$$

$$\tilde{G}_D(n) = B(\beta+n, 2\alpha+2)/B(\beta+1, 2\alpha+2), \quad (23)$$

from which follows

$$\frac{\tilde{G}_U(n)}{\tilde{G}_D(n)} = \frac{\Gamma(\alpha+n)\Gamma(\beta+1)}{\Gamma(\alpha+1)\Gamma(\beta+n)} \equiv \gamma(\alpha, \beta, n). \quad (24)$$

The parameters α and β can now be determined by minimizing

$$C = \sum_{n=2}^N \left[\frac{\gamma(\alpha, \beta, n) - r(n, Q)}{\gamma(\alpha, \beta, n) + r(n, Q)} \right]^2, \quad (25)$$

where N is the maximum number of moments we extract from the CTEQ4LQ data, which we take to be $N=10$. Note that $n=1$ is excluded in Eq. (25), since $\gamma(\alpha, \beta, 1)=1$ is basically due to Eq. (2), and $r(1, Q)=1$ because there are two u_v and one d_v . Varying α and β in search for a minimum in C results in incredibly small C , of the order of 10^{-5} . We find

$$\alpha = 1.755, \quad \beta = 1.05 \quad \text{for } Q = 1 \text{ GeV}/c, \quad (26)$$

$$\alpha = 1.545 \quad \beta = 0.89 \quad \text{for } Q = 10 \text{ GeV}/c. \quad (27)$$

We have not ignored the small Q dependences of α and β since the data on $r(n, Q)$ contain some Q dependence. Moreover, the Q independence of the ratio $\tilde{G}_U(n)/\tilde{G}_D(n)$ does not mathematically preclude the Q dependences of $\tilde{G}_U(n)$ and $\tilde{G}_D(n)$ separately. However, the difference between Eqs. (26) and (27) is not very great, as we can see in Fig. 2, where $G_U(y)$ and $G_D(y)$ are shown [through the use of Eqs. (4) and (5)] for the two extreme Q values, 1 and 10 GeV/c. The

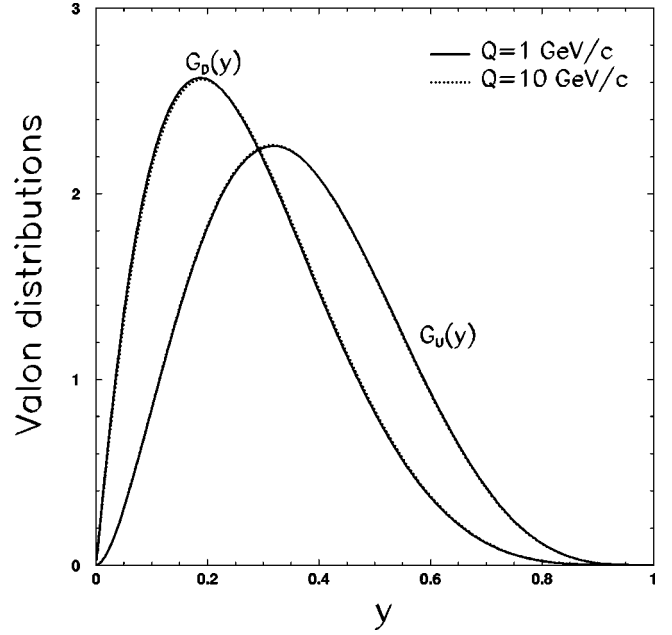


FIG. 2. The U and D valon distributions at two Q values.

difference is insignificant compared to those of the quark distributions, one of which is shown in Fig. 3. With the drastic difference between Figs. 2 and 3 in mind, it is reasonable to conclude that the essence of the valon model has been verified to the extent that the valon distributions exhibit approximate scaling in Q .

It should be remarked that the values of α and β determined above are very different from the ones obtained previously. In Ref. [7] the early data of muon [13] and electron scattering [14] were used in conjunction with a number of theoretical assumptions to yield the values of $\alpha=0.65$ and $\beta=0.35$. In Ref. [11] the modern data of CTEQ4LQ were used, but the values $\alpha=0.70$ and $\beta=0.25$ were obtained due

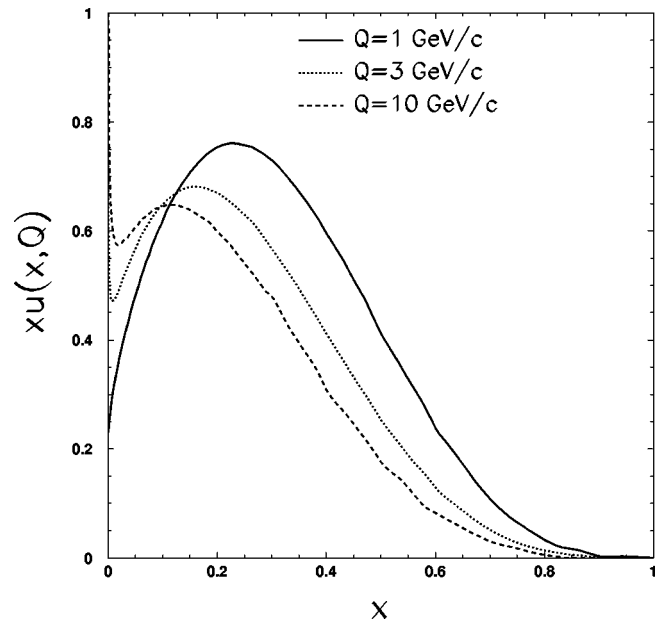


FIG. 3. The u quark distribution functions from Ref. [5].

to the assumption of a specific form of the sea quark distribution (proven to be grossly inaccurate below). Here in this paper we have avoided making any assumption about the sea quark distributions. By extracting the valence quark distributions from CTEQ4LQ we have been able to determine $G_U(y)$ and $G_D(y)$ directly. Clearly, the new values of α and β are more reliable. Further support for their reliability will be given below in connection with the quark distributions u and d , for which our previous parametrization in Ref. [11] has led to unaccountable discrepancies that are unsatisfactory.

From Eq. (13) one sees that the momentum fractions of the valons are given by the $n=2$ moments. From Eqs. (22), (23), (26), and (27), one can then calculate the momentum fractions $\langle y \rangle$, yielding

$$\begin{aligned} \langle y \rangle_U &= 0.3644, & Q = 1 \text{ GeV}/c, \\ \langle y \rangle_U &= 0.3646, & Q = 10 \text{ GeV}/c, \\ \langle y \rangle_D &= 0.2712 & Q = 1 \text{ GeV}/c, \\ \langle y \rangle_D &= 0.2708, & Q = 10 \text{ GeV}/c. \end{aligned} \quad (28)$$

$$\quad (29)$$

At either Q the sum rule

$$2\langle y \rangle_U + \langle y \rangle_D = 1 \quad (30)$$

is satisfied identically. We see that the momentum fractions carried by the valons are essentially independent of Q and that each U valon carries as much as 1.345 times more than the D valon.

IV. THE QUARK AND GLUON DISTRIBUTIONS

Having determined the valon distributions, we can now proceed to the quark and gluon distributions in the valons. From Eq. (16) we have

$$\tilde{K}_{NS}(n, Q) = \tilde{u}_v(n, Q) / 2\tilde{G}_U(n, Q), \quad (31)$$

where we allow $\tilde{G}_U(n, Q)$ to have its weak Q dependence given by Eqs. (26) and (27). Using the moments $\tilde{u}_v(n, Q)$ that we have already calculated from CTEQ4LQ, we obtain the values of $\tilde{K}_{NS}(n, Q)$ as shown in Fig. 4. As expected, $\tilde{K}_{NS}(n, Q)$ undergoes substantial evolution, especially from $Q=1$ to 3 GeV/ c .

To test how good our determination of α and β is, we use the $\tilde{K}_{NS}(n, Q)$ calculated above in conjunction with $\tilde{G}_D(n, Q)$ that can be obtained from Eqs. (5) and (13) so that $\tilde{d}_v(n, Q)$ can be computed using Eq. (17). Note that this computation of $\tilde{d}_v(n, Q)$ requires the knowledge of α and β , while the computation of $\tilde{d}_v(n, Q)$ for the RHS of Eq. (18), i.e., $r(n, Q)$, is based on the CTEQ4LQ data for the RHS of Eq. (20). Our point here is to calculate $d(x, Q)$ from the CTEQ input on $\tilde{u}_v(n, Q)$ in Eq. (31), a procedure that is made possible by the common factor $\tilde{K}_{NS}(n, Q)$ in both Eqs.

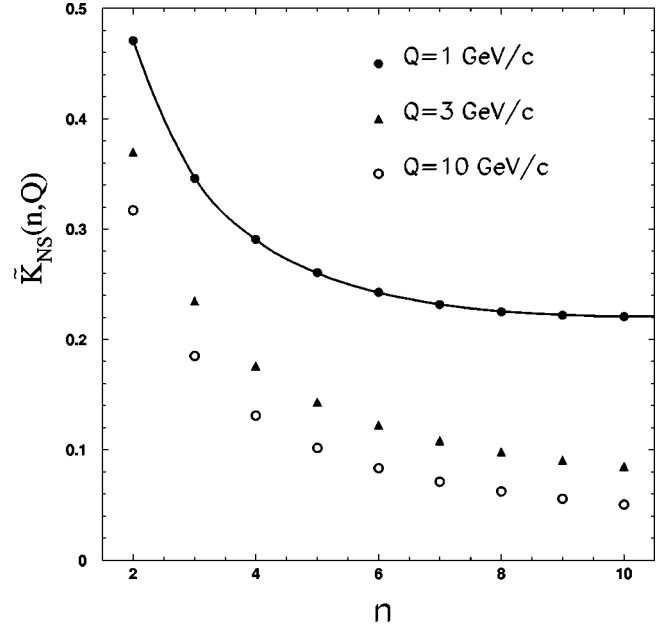


FIG. 4. The moments \tilde{K}_{NS} for three values of Q . The solid line is a fit by Eq. (39).

(16) and (17). Physically, it means that the evolution of quarks in a valon is independent of the flavor of the host valon.

After $\tilde{d}_v(n, Q)$ is obtained by the above procedure that tests the values of α and β , we then make the inverse transform to get the distribution $d_v(x, Q)$. This transform can be facilitated by exploiting the orthogonality of the Legendre polynomials, the details of which are discussed in Ref. [11]. Upon the determination of $d_v(x, Q)$ we can add to it the $\tilde{d}(x, Q)$ distribution from Ref. [5] and obtain $d(x, Q)$. In Fig. 5 we show the u and d quark distributions at $Q=1$ GeV/ c . The solid lines are the distributions posted by CTEQ4LQ [5]. The dotted line for $xd(x)$ is what we have computed using the procedure outlined above. Note that its agreement with the solid line is excellent. The dotted line for $xu(x)$ is essentially the result from fitting the CTEQ4LQ data in the valon model; it merely affirms that the fit is extremely good, so the values of α and β are reliable. The result on $xd(x)$ reveals more about the soundness of the model, since it is not obtained by fitting, but calculated using the valon distribution $G_D(y)$ and the universality of $K_{NS}(z, Q)$.

For the sea quark and gluon distributions, it is for the convenience of the applications of the valon model that we find simple parametrizations of their distributions in a valon. To that end we first write Eqs. (9) and (10) in moment form

$$\tilde{u}(n, Q) = 2\tilde{G}_U(n)\tilde{L}_f(n, Q) + \tilde{G}_D(n)\tilde{L}_u(n, Q), \quad (32)$$

$$\tilde{d}(n, Q) = \tilde{G}_D(n)\tilde{L}_f(n, Q) + 2\tilde{G}_U(n)\tilde{L}_u(n, Q). \quad (33)$$

For the strange quark and gluons, we have

$$\tilde{s}(n, Q) = [2\tilde{G}_U(n) + \tilde{G}_D(n)]\tilde{L}_s(n, Q), \quad (34)$$

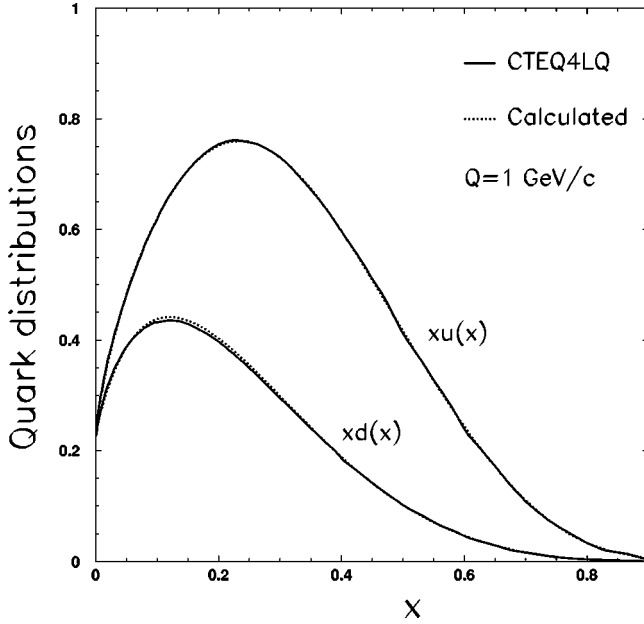


FIG. 5. The u and d quark distribution functions at $Q = 1$ GeV/c. The solid lines are from CTEQ [5]; the dotted lines are calculated in the valon model.

$$\tilde{g}(n, Q) = [2\tilde{G}_U(n) + \tilde{G}_D(n)]\tilde{L}_g(n, Q). \quad (35)$$

Since \tilde{u} , \tilde{d} , \tilde{s} , and \tilde{g} are known from CTEQ4LQ, and \tilde{G}_U and \tilde{G}_D known from Eqs. (22) and (23), we can solve for \tilde{L}_f , \tilde{L}_u , \tilde{L}_s , and \tilde{L}_g . From the result we perform the inverse transform to $L_f(z, Q)$, $L_u(z, Q)$, $L_s(z, Q)$, and $L_g(z, Q)$, respectively. These distributions are shown in Figs. 6 and 7, for $Q = 1, 3$, and 10 GeV/c. Being in log-log plots, the evolutions due to the changes in Q are substantial, as expected.

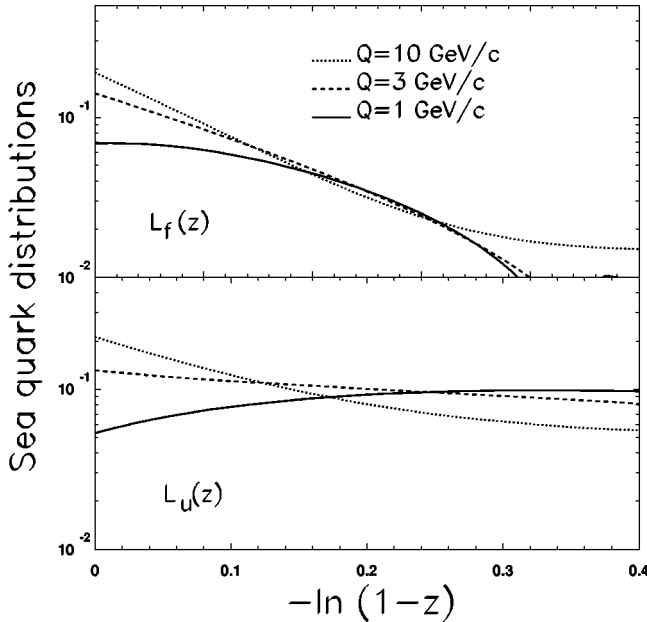


FIG. 6. The favored and unfavored sea quark distributions in the valon at three values of Q .

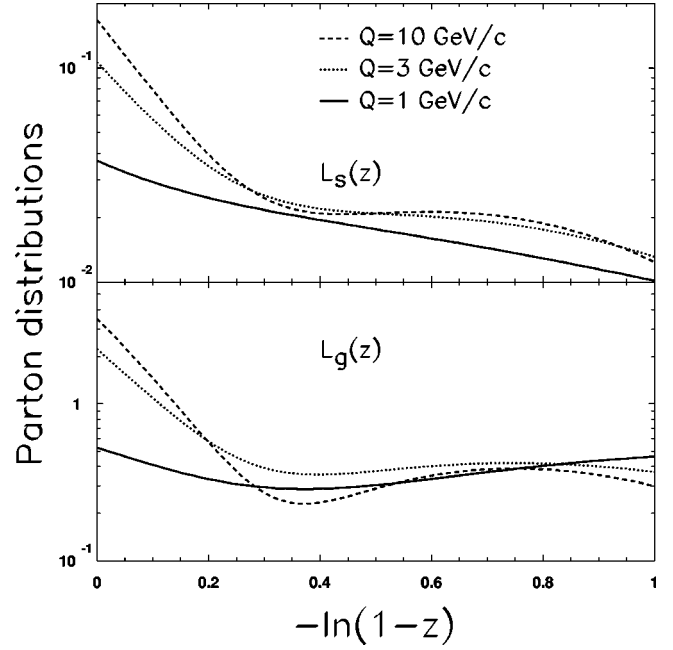


FIG. 7. The strange quark and gluon distributions in the valon at three values of Q .

What we have not expected is the drastic difference between $L_f(z, Q)$ and $L_u(z, Q)$. For $0 < -\ln(1-z) < 0.4$, the range of z is $0 < z < 0.33$. For $z > 0.4$ we find that $L_f(z, Q) \ll L_u(z, Q)$, at least for $Q = 1$ and 3 GeV/c. At higher Q the evolution can generate more favored sea quarks. Thus at low Q , where sea quarks are few, Pauli blocking suppresses the favored sea quarks so much at high z that the unfavored sea quarks dominate. Indeed, our calculation of $L_f(z, Q)$ is unreliable for $z > 0.4$ because from the finite number of moments ($n < 10$) that were taken the inverse transform generates oscillations in z at high z . There is no such problem with the s quark and gluon distributions, as is evident in Fig. 7, since they are not inhibited by Pauli blocking. The general property is that all the parton distributions increase significantly at small z , when Q is increased.

There is no simple way to describe both the z and Q dependences of the parton distributions. In order for the valon model to be useful, especially in applications to the study of inclusive cross sections in hadronic collisions at low p_T , an analytic description of each of the parton distributions is needed. For such problems only the distributions at $Q = 1$ GeV/c are relevant, so we fit those distributions by polynomials. The formula used for the fitting is

$$\ln L_i(z, Q=1) = \sum_{j=0}^3 a_j^{(i)} t^j, \quad t = -\ln(1-z). \quad (36)$$

The result of the fitting is shown in Fig. 8, for which the values of the coefficients are given in Table I. The fits are evidently very good. Thus we have completely specified the PDFs at $Q = 1$ GeV/c in analytical and numerical ways, suitable for transport to problems where such PDFs are needed.

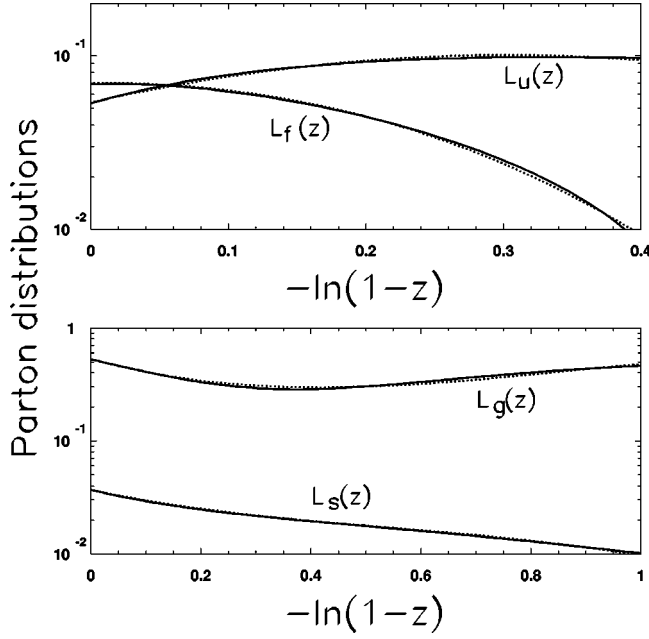


FIG. 8. Fits of the f, u, s , and g distributions at $Q=1$ GeV/c, as shown by the dotted lines.

In applications, such as in Ref. [11], the moments are more useful than the PDFs themselves. We show the moments at $Q=1$ GeV/c in Fig. 9, together with their fits. The fitting is done mainly for the convenience of applications. The formula used for fitting is

$$\ln \tilde{L}_i(n) = - \sum_{j=0}^3 b_j^{(i)} u^j, \quad u = \ln(n-1), \quad (37)$$

where the coefficients are given in Table II.

The rapid decrease of the favored quark moments $\tilde{L}_f(n)$ with increasing n is now very evident, while the other three parton moments have roughly similar n dependences.

It is important to check the momentum sum rule of the partons. We have seen in Eq. (30) that the valon momentum fractions add up to 1; now the parton momentum fractions in each valon must also add up to 1. Since $\tilde{K}_{NS}(z)$ and $L_i(z)$ are invariant distributions, their moments at $n=2$ are their momentum fractions. We therefore should have

$$\tilde{K}_{NS}(2) + \tilde{L}_g(2) + 2 \sum_{i=f,u,s} \tilde{L}_i(2) = 1. \quad (38)$$

We have $\tilde{K}_{NS}(2) = 0.4707$ at $Q=1$ GeV/c, and from Table II we can calculate $\tilde{L}_i(2) = \exp[-b_0^{(i)}]$, yielding 0.0162,

TABLE I. Coefficients in Eq. (36).

i	$a_0^{(i)}$	$a_1^{(i)}$	$a_2^{(i)}$	$a_3^{(i)}$
f	-2.66	0.08	-10.4	-6.0
u	-2.92	4.0	-5.95	-1.4
s	-3.30	-2.4	2.7	-1.65
g	-0.63	-3.1	4.9	-1.9

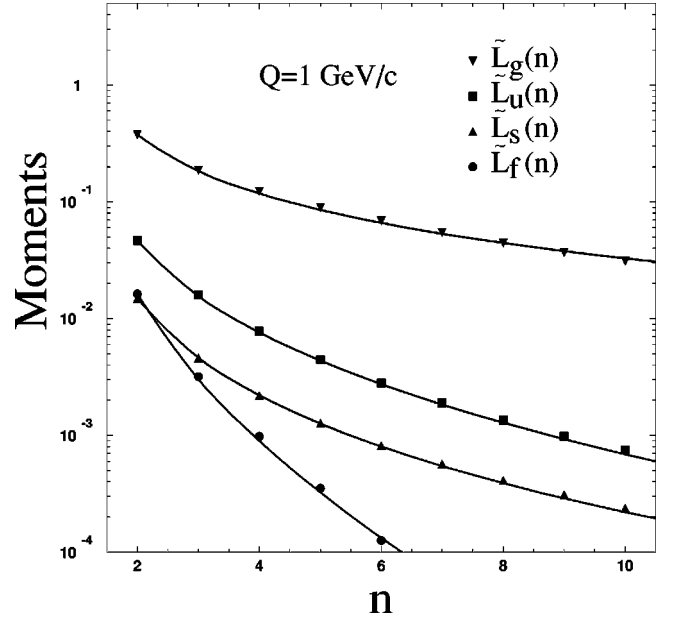


FIG. 9. The moments $\tilde{L}_g(n), \tilde{L}_u(n), \tilde{L}_s(n)$, and $\tilde{L}_f(n)$ at $Q=1$ GeV/c and their fits.

0.0465, 0.0148, and 0.3754 for $i=f, u, s$, and g , respectively. According to the LHS of Eq. (38) they sum up to 1.001, an excellent confirmation of the momentum sum rule.

As a final item of parametrizing the moments of the parton distributions, we also give here a formula that fits $\tilde{K}_{NS}(n, Q)$ at $Q=1$ GeV/c,

$$\ln \tilde{K}_{NS}(n) = - \sum_{j=0}^3 c_j u^j, \quad (39)$$

where $c_j = 0.753, 0.401, 0.0962$, and 0.0555 , for $j=0, 1, 2$, and 3 , respectively. The solid line in Fig. 4 shows the fit.

V. CONCLUSION

We have shown that the PDFs in a proton can be described in two stages: valons in a proton and then partons in a valon. The valon distribution functions are essentially independent of Q , while the parton distributions in the valons are Q dependent. The three valons carry all the momentum of the proton, and the way that the parton momenta are distributed in a valon is independent of the host valon so long as the sea quark flavors are identified as favored or unfavored, instead of by specific flavors like u or d . We have found that Pauli blocking significantly suppresses the favored quarks

TABLE II. Coefficients in Eq. (37).

i	$b_0^{(i)}$	$b_1^{(i)}$	$b_2^{(i)}$	$b_3^{(i)}$
f	4.12	2.2	0.2	0.18
u	3.07	1.5	0.08	0.05
s	4.21	1.6	0.1	0.02
g	0.98	1.0	0.05	0

compared to the unfavored quarks. At $Q=1$ GeV/ c , the valence quarks carry 47.1% of the proton momentum, while the gluons carry 37.5%. The scaling behavior of the valon distributions and the universality of the valon structure give support to the valon model as a simple and organized description of the nucleon structure.

We have determined the parameters in simple formulas that adequately describe the parton distributions (and their moments) in a valon at $Q=1$ GeV. This is done for the benefit of applications of the valon model to low- p_T hadronic reactions that are not perturbative. Such distributions are needed when the parton degrees of freedom are released. If in some nuclear reactions at some energy the partons do not exhibit their dynamical effect beyond the valons, as suggested by Csörgő [15] for heavy-ion collisions at CERN-SPS, then the valon distributions are all that is needed. Since the exclusive valon distribution is the absolute square of the wave function of the proton in the valon representation, it is also the recombination function of valons in forming a proton [6]. Thus the new values of α and β found here affect the calculation of hadron production at low p_T .

The valon model can, of course, also be applied to other hadrons beside the proton. Although the data on the PDFs of the pion or the kaon are not of the same quality as those of

the proton, some data on the Drell-Yan and prompt photon production initiated by mesons do exist. It will be a natural extension of this work to determine the valon distributions in the mesons by using the PDFs obtained from such a data. By virtue of the universality of the parton distributions in valons, what we have found here from the proton is good enough for the mesons also.

The affirmation of the validity of the valon model makes possible a logical link between the bound-state problem of the hadrons in terms of the constituent quarks and the scattering problem in terms of the partons. The relationship between the wave functions of the constituent quarks and the valon distributions was studied in the context of form factors [16]. In view of the new distributions determined here, that problem needs to be revisited. On the whole, our understanding of the hadron structure problem is enhanced by our study here of the modern parton distribution functions in the framework of the valon model.

ACKNOWLEDGMENTS

We are grateful to D. Soper for helpful comments. This work was supported, in part, by the U.S. Department of Energy under Grant No. DE-FG03-96ER40972.

-
- [1] H.L. Lai *et al.*, CTEQ Collaboration, Phys. Rev. D **51**, 4763 (1995); **55**, 1280 (1997).
 - [2] A.D. Martin, W.J. Stirling, and R.G. Roberts, Phys. Rev. D **47**, 867 (1993); **50**, 6734 (1994).
 - [3] M. Glück, E. Reya, and A. Vogt, Z. Phys. C **53**, 127 (1992).
 - [4] G. Sterman *et al.*, Rev. Mod. Phys. **67**, 157 (1995).
 - [5] CTEQ4LQ, <http://zebu.uoregon.edu/~parton/partongraph.html>
 - [6] R.C. Hwa, Phys. Rev. D **22**, 759 (1980).
 - [7] R.C. Hwa and M.S. Zahir, Phys. Rev. D **23**, 2539 (1981).
 - [8] K.P. Das and R.C. Hwa, Phys. Lett. **68B**, 459 (1977).
 - [9] R.C. Hwa, Phys. Rev. D **22**, 1593 (1980).
 - [10] R.C. Hwa and C.B. Yang, Phys. Rev. C **66**, 025205 (2002), following paper.
 - [11] R.C. Hwa and C.B. Yang, Phys. Rev. C **65**, 034905 (2002).
 - [12] M. Arneodo *et al.*, New Muon Collaboration, Phys. Rev. D **50**, R1 (1994).
 - [13] B.A. Gordon *et al.*, CHIO Collaboration, Phys. Rev. D **20**, 2645 (1979).
 - [14] A. Bodek *et al.*, Phys. Rev. D **20**, 1471 (1979); W.B. Atwood *et al.*, Phys. Lett. **64B**, 479 (1976).
 - [15] T. Csörgő, Nucl. Phys. B (Proc. Suppl.) **92**, 62 (2001).
 - [16] R.C. Hwa and C.S. Lam, Phys. Rev. D **26**, 2338 (1982).